ELSEVIER
Journal of Atmospheric and Solar-Terrestrial Physics 65 (2003) 1329–1335
Journal of ATMOSPHERIC AND SOLAR-TERRESTRIAL PHYSICS
www.elsevier.com/locate/jastp

The signature of short-period gravity waves imaged in the OI 557.7 nm and near infrared OH nightglow emissions over Panhala

G.K. Mukherjee*

Indian Institute of Geomagnetism, Navi Mumbai 410218, India

Abstract

With the development of cooled CCD detector, it has become possible to detect the spatial and temporal variation of the small-scale structure in airglow emission more accurately. Using tilting filter photometers (630 nm and OH) and a CCD-based multi-channel all-sky imager, the night airglow observations were carried out from Kolhapur (16.8°N, 74.2°E) and Panhala (17.0°N, 74.2°E; height above mean sea level 3200 ft), India, during the clear and moonless nights of January–February, 2001. The multi-wavelength airglow imaging enables us to study the horizontal structures of the small-scale gravity waves at various heights in the region of emissions and to investigate propagation of those waves in detail. Hydroxyl (OH) and OI 557.7 nm images on the night of February 18, 2001 showed row-like structures moving from north to south direction spanning over 500 km in the sky. The observed horizontal phase speed (∼50 m/s), wavelength (∼25 km), wave period (∼8 min) of the atmospheric gravity waves have been determined from a set of sequential images of OI 557.7 nm (at 97 km) and OH (at 86 km) observed at Panhala. These are the first observation of the signature of atmospheric gravity waves using an all-sky imager in Indian region indicating perturbation in density in the mesospheric region (80–100 km). The possible sources of the waves to the extended region have been discussed.

Keywords: Gravity waves; Airglow emission; All-sky imager; Mesosphere

1. Introduction

Short-period gravity waves with wavelengths from a few kilometers to a few hundred kilometers have been extensively studied at low-, mid- and high-latitude regions (Shiokawa et al., 2000 and references there in). With the advent of charge coupled devise (CCD) based all-sky imagers, it has been possible to measure the intensity of emission of various airglow lines more accurately. Typical altitudes of observation of gravity waves were confined to 80–100 km, the mesopause layer using the infrared OH, the visible OI 557.7 nm and Na emission lines (Taylor and Garcia, 1995). As the gravity waves with the origin in the troposphere carry energy and momentum to the region between the mesopause and the lower thermosphere, they are very important for studying the dynamics of the region. When gravity waves propagate through airglow layers, the atoms or molecules and ions, cause photochemical reactions also, fluctuate. As a result, airglow intensity is perturbed and layers show two-dimensional wave pattern. Through airglow imaging temporal and spatial structure of gravity waves can be inferred. The airglow structure can be interpreted as the result of waves passing through the airglow layer and so we can use this data to determine the horizontal wavelength and phase velocity of the waves (Swenson and Mende, 1994). Note that since the airglow emission originates from a fairly thin layer, the image data allows us to see a horizontal slice through the three-dimensional gravity wave pattern when they are moving from tropopause to the mesosphere.

* Tel.: +91-22-27480768; fax: +91-22-27480762.
E-mail address: gkm@iig.iigm.res.in (G.K. Mukherjee).

1364-6826/$ - see front matter
doi:10.1016/j.jastp.2003.08.013

Table 1
Filter details and exposure times for the all-sky imager

Emission	Wavelength	Diameter of the filters (in)	Band width (nm)	Transmission (%)	Integration time (s)
OI 557.7 nm	OI 557.7 nm	4	1.0	65	60
OH bands	OH 720–910 nm[a]	4	190	65	15

[a] With a notch at 865 nm to suppress O_2 (0,1) emission.

Using CCD-based all-sky imager, multi-point observations of short-period gravity waves were carried out in Japan over an extended area (Shiokawa et al., 2000). Three all-sky cameras were used to measure OH airglow at three stations in Japan which were separated by distances of 250 –1300 km. Similar wave structures, characterized by horizontal wavelengths of 20–40 km and northward phase velocity of 20–40 m/s, were observed at all three stations indicating that the spatial extension of the short-period waves was more than 1000 km. Taylor and Garcia (1995) applied two-dimensional spectral techniques and interpreted a set of image data (OH and OI 557.7 nm) that consisted of two intersecting quasi-monochromatic gravity wave patterns progressing on approximately orthogonal headings. Though there are plenty of observations of gravity waves through the airglow images from other parts of the globe showing horizontal wavelengths ranging between 5 and 100 km (Clairemidi et al., 1985; Armstrong, 1986; Nakamura et al., 1999; Shiokawa et al., 1999; Taylor et al., 1995, 1997, 1998; Prusa et al., 1996), the observations were not available from the Indian region due to absence of a suitable imaging system.

In this report, we present the first observation of short-period gravity waves using an all-sky camera from India from the top of a hill at Panhala and discuss the characteristic parameters for two typical events and possible sources of these waves.

2. Instrumentation and theory of tropical emissions

The design of a CCD-based imaging system has been discussed, amongst others, by Baumgardner and Karandanis (1984), Mendillo et al. (1989) and more recently by Mendillo et al. (1997), Mukherjee et al. (1998), Nakamura et al. (1999) and Kubota et al. (2001). The all-sky imager that we used for observation was developed in collaboration with Boston University, US. This has six filters on a wheel, a fish-eye lens that has a field of view of 180° and an intensified cooled CCD camera with 384 × 256 pixels. The various emission lines originating at different ionospheric/thermospheric and mesospheric heights can be studied almost simultaneously with the help of this system. In this report, we present the results using two filters: OI 557.7 nm and OH. The details about the filters and the exposure time used are given in Table 1.

The major portion of OI 557.7 nm emission comes from the recombination of oxygen atoms in the mesopause region (80–100 km). There is a general agreement that the OI 557.7 nm emission is excited by the so-called two-step energy transfer process: $O + O + M \rightarrow O_2^* + M, O_2^* + O \rightarrow O(^1S) + O_2$. A part of this emission also originates from the dissociative recombination process in the F region. The later contribution is estimated to be about 20% of the OI 630 nm emission in the F region (Sobral et al., 1992).

The Meinel band hydroxyl emits radiation so that the excited hydroxyl radicals (OH*) immediately transfer to the lower stable energy level. OH* is considered to be produced by the following reactions:

$$O_3 + H \rightarrow OH^*(v \leqslant 9) + O_2,$$

$$HO_2 + O \rightarrow OH^*(v \leqslant 6) + O_2,$$

$$O_2^* + H \rightarrow O + OH^*,$$

$$OH^*(v) \rightarrow OH^{**}(v') + h\nu(550\ \text{nm} - 4.4\ \mu\text{m}),$$

where * and ** indicate that the molecule is in the state of excitation, and v and v' indicate the order of states of molecules. The peak altitudes of the OH and OI 557.7 nm emission layers were observed to be ~86 and ~97 km, respectively, with a layer width of ~11 km each (Kubota et al., 1999).

3. Image analysis and results

Fig. 1 shows the location of the observing station Panhala with respect to geographic coordinates. The two circles indicate the coverage of the camera system for zenith distances 75° and 90° for mesospheric emission height of 90 km at Panhala. The all-sky imager was operated from Panhala hill during January and February 2001 on clear moonless nights to detect the signature of gravity waves. Despite the extended period of observations, we could detect very few events with signatures of gravity waves in OI and OH images. This could be due to the resolving power of the CCD camera with 384 × 256 pixels. Therefore, we discuss only two typical representative gravity wave events in this short report. In an hour, 14 images were obtained for OI 557.7 nm and OH emissions. The fish-eye lens image is transformed into the image in the geographic co-ordinates,

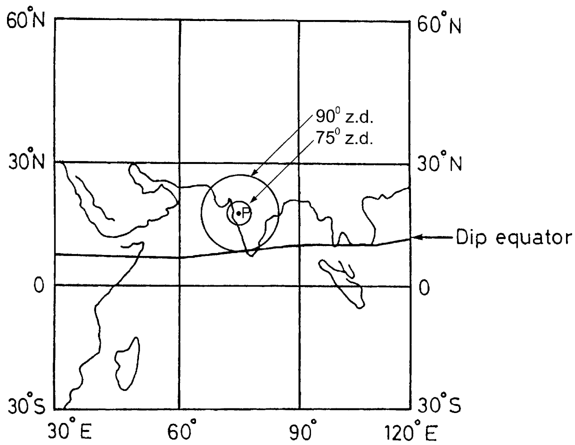

Fig. 1. Field of view at 75° and 90° zenith angles at mesospheric emission height of 90 km for the all-sky camera at Panhala.

by assuming emission height of 86 km for OH and 97 km for OI 557.7 nm emission. The mean image is obtained by averaging together a series of 14 images (obtained in 1 h) processed through IDL software (Kubota et al., 1999). The mean processed image was used to flat field the image data set. The non-uniformity of all-sky images due to van Rhijn effect, the atmospheric extinction, and the non-uniform sensitivity of the imager are corrected roughly by this process. Fig. 2 shows the processed images. The upper panel in the figure shows that at the center of the OI 557.7 nm image at 2138, 2142 and 2146 h IST on February 18, 2001, the distinct wave structures aligned in east–west direction are seen, which are considered to be modulation of airglow layer by gravity waves. These small-scale structures were intersecting the north–south aligned structures observed in the images, which are due to contributions from ionospheric F region plasma bubbles (depletion in intensity) moving eastward. The lower panel displays the similar east–west aligned signature of gravity waves in hydroxyl OH airglow at 2136, 2140 and 2144 h IST. The disturbances were detected both in the OI and OH layers (mean separation ∼11 km) suggesting that wave energy was able to propagate from the mesosphere into the lower thermosphere. Using the geographical coordinates and height of the layer of emission and geometry, different characteristic parameters (phase velocity, wavelength, direction of propagation, period, etc.) of gravity waves were determined. In order to get the parameters a portion of the image, rectangular in size, is cut out from both OH and OI 557.7 nm images. For calculation of distances from zenith in geographical coordinates, the height of the emission layer for OH and OI 557.7 nm have been assumed to be 86 and 97 km (Kubota et al., 1999). It is evident from both Figs. 3 and 4 that the waves propagate initially towards southwest direction between 21:04 and 21:33 h IST and, subsequently, thereafter the waves propagated almost in the meridional direction to the south. The waves were only observed for 1 h and 10 min between 21:00 and 22:10 h. The horizontal wavelength and the direction of propagation of isophase lines are determined from the figures and the horizontal phase speed have been derived from a set of successive images of OH and OI 557.7 nm, then the wave period was determined (Nakamura et al., 1999). The horizontal wavelength in the meridional direction,

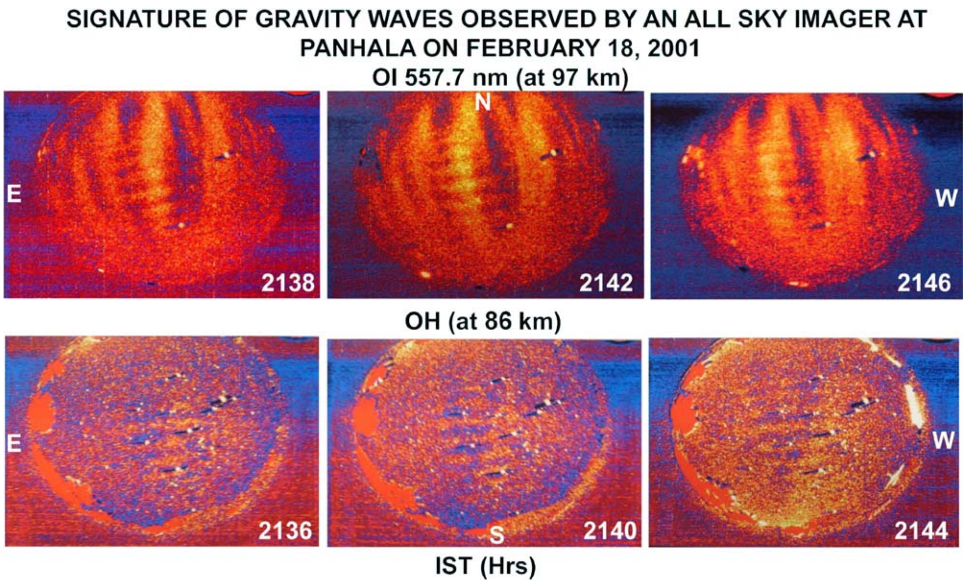

Fig. 2. All-sky images of OI 557.7 nm and OH airglow images showing row like structures (east–west) of gravity waves obtained at Panhala on the night of February 18, 2001. The indicated timings are in IST (IST = UT + 5.5 h).

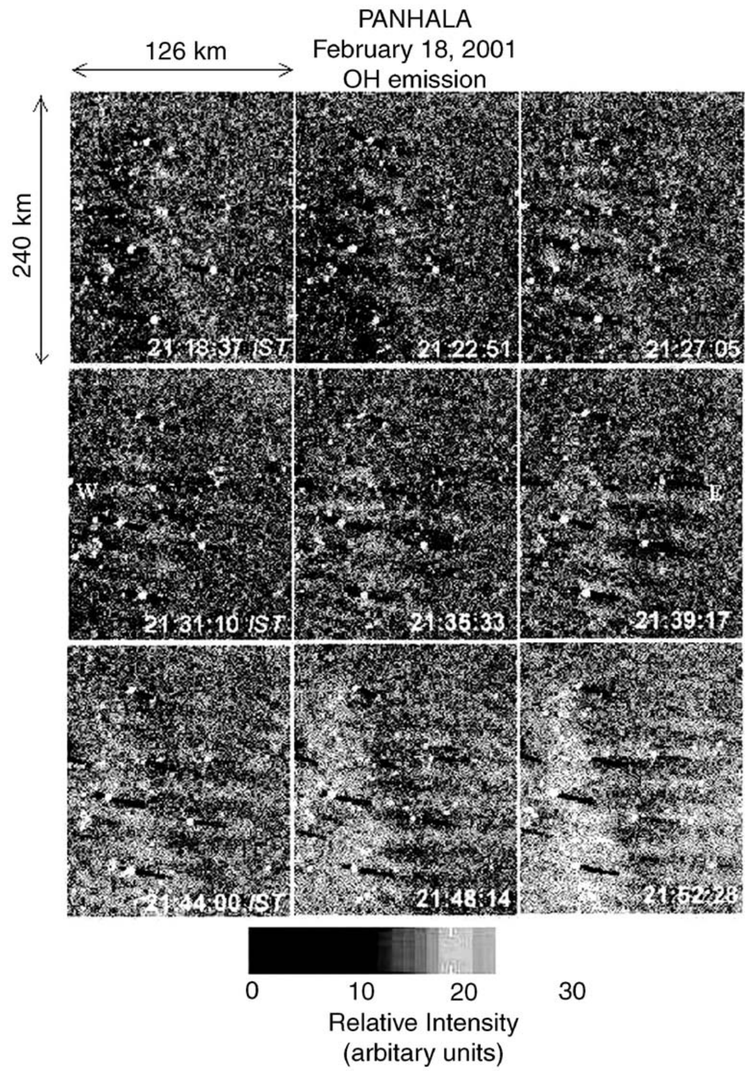

Fig. 3. Set of images showing quasi-monochromatic gravity wave patterns imaged on February 18, 2001 in the OH emission in geographic coordinates from 21:00 to 22:00 h IST.

corresponding to the band separation in their southward movement, is estimated to be about 25 km. The phase velocities of the wave fronts are estimated to be about 50 m/s. It was inferred that the short-period (∼8 min) gravity waves with 25 km wavelength were dominant at the sky of Panhala during 2100–2210 h IST which were spread over spatial scale of ∼500 km.

A tilting photometer unit (Mukherjee and Dyson, 1992) was also operational at a near by place, 20 km away from Panhala at Kolhapur. Fig. 6 shows the zenith intensity variation of OI 630 nm and OH (8,3) intensity obtained at Kolhapur during the night of February 18, 2001. It is clearly seen that the intensity of the OI 630 nm emission increases with local time reaching its maximum value around midnight while that of OH Meinel bands decreases during the same period. The relative intensity variations are much larger for OI 630 nm emission than for OH (8,3). The figure also shows small fluctuations in OH airglow.

In Fig. 5, we show another typical example of the signature of gravity waves in OH images observed on the night of January 22, 2002 at Panhala between 21:00 and 22:00 h. These images depict the propagation direction of gravity waves from northwest to southeast direction. The large-scale band structure moves with a velocity 60 m/s towards southeast direction. Assuming an emission height of 86 km in the OH images, the average horizontal wavelength of the structure is found to be ∼40 km. The structure is clearly seen in OH images but remains absent in OI images.

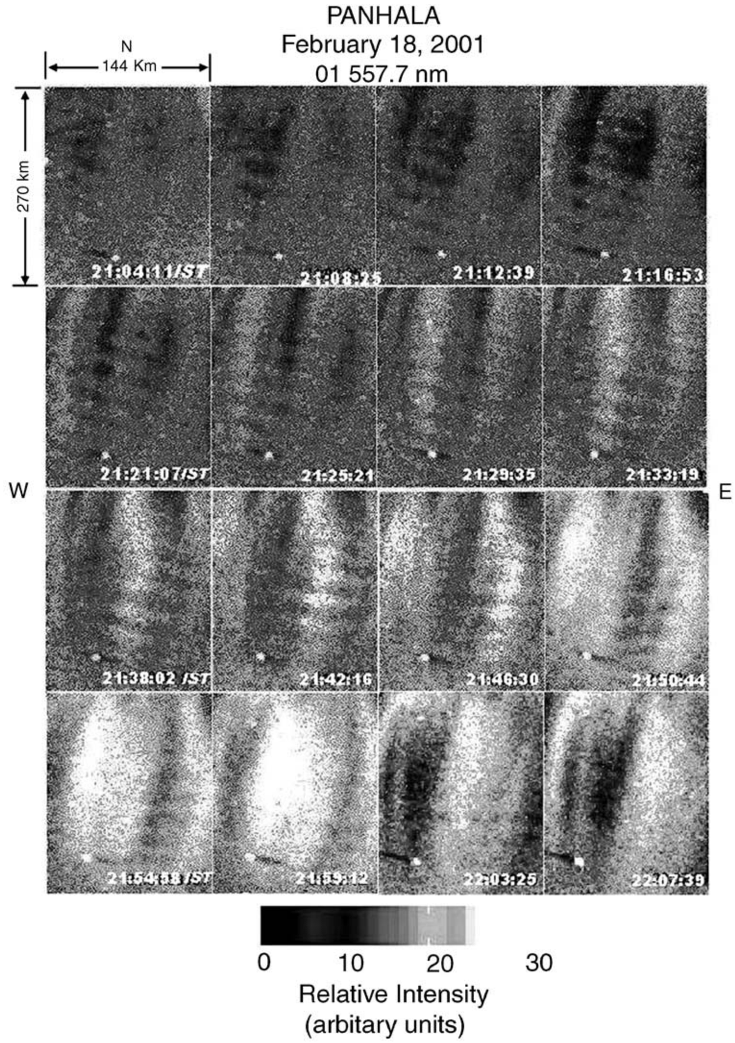

Fig. 4. Same as Fig. 3 but for OI 557.7 nm emission images.

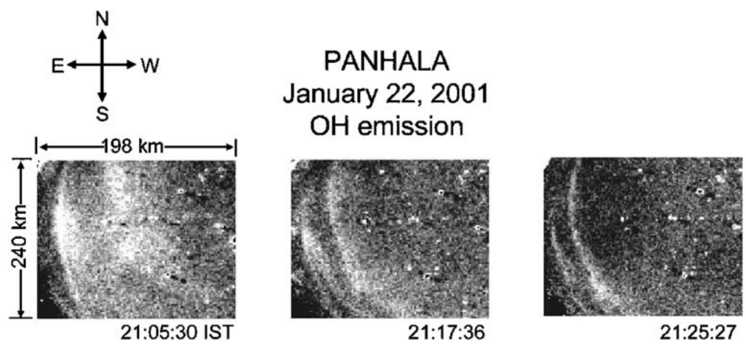

Fig. 5. Plot showing the band type gravity wave pattern in OH images on the night of January 22, 2001 at Panhala propagating in southeast direction.

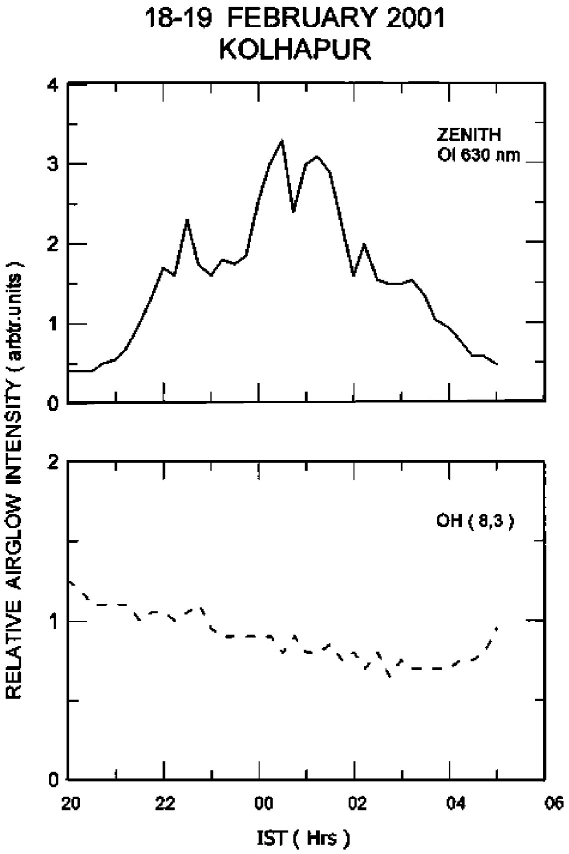

Fig. 6. Plot showing the photometric intensity variation of OI 630 nm emission and OH (8,3) on the night of February 18/19, 2001 observed at Kolhapur.

4. Discussion and conclusions

Atmospheric gravity waves play an important role in the dynamics and energetics in the mesosphere and lower thermosphere. Wave-like structures of gravity waves were detected in the images of OI 557.7 nm and hydroxyl OH emissions on the night of February 18, 2001 when an all-sky imager was operated from the top of a hill at Panhala in India. These are the first imaging observation of gravity waves from Indian low-latitude region. The characteristic features of the observed gravity waves are summarized below:

Short-period gravity waves with wavelengths 25 km have been observed at Panhala on February 18, 2001 during 2100 –2200 h, they were spread over a region of ~500 km. They were initially moving to southwest and then southward with a phase velocity of 50 m/s. The average K_p index for the day was 1 and the average decimetric solar flux indices (F 10.7 cm) for the day was 129 units (10^{-22} W/m^{-2}). It was geomagnetically quiet period with low solar activity. Both the disturbances were detected in the OH and OI layers (mean separation ~11 km) suggesting that wave energy was able to propagate from the mesosphere into the lower thermosphere over a very large region. This is also inferred from the phases of the wave propagation at two altitudes and the fading of the waves from lower to higher altitudes. The results have implications on the sources of these waves. The gravity waves are classified broadly into two types; bands and ripples. The ripples have wavelengths of 5–15 km and are short lived (< 45 min) with restricted spatial coverage. On the other hand, the bands are large and having long-lasting wave patterns with horizontal wavelengths of several tens of km. The band structure of the gravity waves have been commonly studied and reported through airglow imaging because of their long-lasting nature.

The linear dispersion relation of the gravity wave is expressed as (Hines, 1960)

$$m^2 = (N^2/(u-c)^2) - k^2 - 1/4H^2, \tag{1}$$

where m, N, u, c, k and H are the vertical wave number, Brunt–Väisärä frequency, background wind velocity, observed wave phase velocity, horizontal wave number and scale height, respectively. The vertical (V_{gz}) and horizontal (V_{gx}) group velocity of the waves are derived from $V_{gz} = \partial\omega/\partial m$ and $V_{gx} = \partial\omega/\partial k$ (where the wave frequency, $\omega = ck$) to give (Shiokawa et al., 2000)

$$V_{gz} = \pm Nmk/(m^2 + k^2 + 1/4H^2)^{3/2}, \tag{2}$$

$$V_{gx} = u \pm N(m^2 + 1/4H^2)/(m^2 + k^2 + 1/4H^2)^{3/2}. \tag{3}$$

Eqs. (2) and (3) give the vertical and horizontal group velocities of wave energy propagation. It is seen that the vertical propagation of gravity waves is strongly influenced by horizontal wind velocity in the background.

We do not have horizontal wind profile at the place of imaging observation; therefore, we assume $u = 0$. The values of c and k have been estimated from the airglow measurement (February 18, 2001) as ~50 m/s and $\sim 2\pi/25$. In the atmosphere, the vertical propagation to be possible, $\omega^2 < N^2$. The realistic value of $N \sim 0.02$ rad/s has been assumed to compute the vertical wavelength and vertical group velocities. This corresponds to relaxation time $(2\pi/N) \sim 5$ min for the average atmosphere. However, $u = 0$ and $N = 0.02$ are too simplified background conditions and the wave propagation from the troposphere/tropopause is just one example of the possible case. The vertical wavelength, $L_v = 2\pi/m$, and the horizontal and vertical group velocities of the observed waves are computed to be ~20 km, $\sim \pm 30$ m/s and $\sim \pm 22$ m/s. As the waves were observed over a very large area localized in the mesosphere, it is unlikely that the sources of the waves were localized. There is a possibility that if the source region is localized in the area but the wave is ducted in the MLT region and propagated horizontally, it is possible to have large horizontal extent. Tropospheric disturbances, such as thunder storms, fluid instabilities, collapse of fronts, localized shear (vortices) can generate large-scale gravity waves. However, the background wind data from Radar can confirm and give useful information about the distribution of the source region and the propagation of the gravity waves.

Acknowledgements

The author is grateful to Dr. Toshitaka Tsuda and Dr. T. Nakamura of Radio Science Centre for Space and Atmosphere (RASC), Kyoto University, Uji, Japan for useful discussions on atmospheric gravity waves during the author's visit to RASC under JSPS fellowship.

The all-sky camera has been developed with the collaboration of Prof. M. Mendillo and his group at Boston University, Boston, USA. The author is grateful to Prof. M. Mendillo for his continued interest in the project. Department of Science and Technology (DST), Government of India, New Delhi, fund the research in upper atmospheric sciences at IIG. The all-sky imager was operated from Panhala with the technical support of Mr. P.T. Patil and Mr. S.H. Mahajan. The nightglow observations at Kolhapur and Panhala were carried out under scientific collaboration program between IIG, Mumbai and Shivaji University, Kolhapur.

References

Armstrong, E.B., 1986. Irregularities in the 80–100 km: a Photographic Approach. Radio Science 21, 313–317.

Baumgardner, J., Karandanis, S., 1984. CCD system using video graphics controller. Electronic Imaging 3, 28–31.

Clairemidi, J., Herse, M., Moreels, G., 1985. Bi-dimensional Observation of Waves Near the Mesopause at Auroral Latitudes. Planetary and Space Sciences 33, 1013–1022.

Hines, C.O., 1960. Internal atmospheric gravity waves at ionospheric height. Canadian Journal of Physics 38, 144–148.

Kubota, M., Ishi, M., Shiokawa, K., Ejiri, M.K., Ogawa, T., 1999. Height measurements of nightglow structures observed by all-sky imagers. Advances in Space Research 24, 593–596.

Kubota, M., Fukunishi, H., Okano, S., 2001. Characteristics of medium- and large-scale TIDs over Japan derived from OI 630-nm nightglow observation. Earth Planets Space 53, 741–751.

Mendillo, M., Baumgardner, J., Sultan, P.J., 1989. Optical and radar techniques applied to chemical release in active experiments in the ionosphere/thermosphere system. Advances in Space Research 10, 8–15.

Mendillo, M., Baumgardner, J., Colerico, M., Nottingham, D., 1997. Imaging science contributions to equatorial aeronomy: initial results from the MISETA program. Journal of Atmospheric and Terrestrial Physics 59, 1587–1599.

Mukherjee, G.K., Dyson, P.L., 1992. A filter tilting photometer for nightglow measurement of 630.0 nm emission line. Indian Journal of Radio and Space Physics 21, 212–217.

Mukherjee, G.K., Carlo, L., Mahajan, S.H., Patil, P.T., 1998. First results of all-sky imaging from India. Earth Planets Space 50, 119–127.

Nakamura, T., Higashikawa, A., Tsuda, T., Matsushita, Y., 1999. Seasonal variation of gravity wave structures in OH airglow with a CCD imager at Shigaraki. Earth Planets Space 51, 897–906.

Prusa, J.M., Smolarkiewicz, P.K., Garcia, R.R., 1996. Propagation and breaking at high altitudes of gravity waves excited by tropospheric forcing. Journal of Atmospheric Sciences 53, 2186–2216.

Shiokawa, K., Katoh, Y., Satoh, M., Ejiri, M.K., Ogawa, T., Nakamura, T., Tsuda, T., Wiens, R.H., 1999. Development of optical mesosphere–thermosphere imagers (OMTI). Earth Planets Space 51, 887–896.

Shiokawa, K., Ejiri, M.K., Otsuka, Y., Ogawa, T., Kubota, M., Igarashi, K., Saito, A., Nakamura, T., 2000. Multipoint observations of short period waves over Japan during the Front campaign. Geophysical Research Letters 27, 4057–4060.

Sobral, J.H.A., Takahashi, H., Abdu, M.A., Muralikrishna, P., Sahai, Y., Zamlutti, C.J., 1992. O (^{1}S) and O (^{1}D) quantum yields from rocket measurements of electron densities and 557.7 and 630 nm emissions in the nocturnal F region. Planetary and Space Sciences 40, 607–619.

Swenson, G.R., Mende, S.B., 1994. OH emission and gravity waves (including a breaking wave) in all-imagery from Bear Lake, UT. Geophysical Research Letters 21, 2239–2242.

Taylor, M.J., Garcia, F.J., 1995. A two dimensional spectral analysis of short period gravity waves imaged in the OI (557.7 nm) and near infrared OH nightglow emissions over Arecibo, Puerto Rico. Geophysical Research Letters 22, 2473–2476.

Taylor, M.J., Bishop, M.B., Taylor, V., 1995. All-sky measurements of short period waves imaged in the OI (557.7 nm), Na (589.3 nm) and near infrared OH and O_2 (0,1) airglow emissions during the ALOHA-93 campaign. Physical Research Letters 22, 2833–2836.

Taylor, M.J., Pendleton, W.R., Clark Jr., S., Takahashi, H., Gobbi, D., Goldberg, R.A., 1997. Image measurements of short period gravity waves at equatorial latitudes. Journal of Geophysical Research 102, 26283–26299.

Taylor, M.J., John, J.M., Fukao, S., Saito, A., 1998. Possible evidence of gravity wave coupling into the mid latitude ionosphere during the SEEK campaign. Geophysical Research Letters 25, 1801–1802.